ACS APPLIED MATERIALS & INTERFACES

Research Article

www.acsami.org

Digital Memory Versatility of Fully π-Conjugated Donor–Acceptor Hybrid Polymers

Yong-Gi Ko,[†,§] Dong Min Kim,[†,§] Kyungtae Kim,[†] Sungmin Jung,[†] Dongwoo Wi,[†] Tsuyoshi Michinobu,*[,‡] and Moonhor Ree*[,†]

[†]Department of Chemistry, Division of Advanced Materials Science, Center for Electro-Photo Behaviors in Advanced Molecular Systems, Pohang Accelerator Laboratory, Polymer Research Institute, and BK School of Molecular Science, Pohang University of Science & Technology (POSTECH), Pohang 790-784, Republic of Korea

[‡]Department of Organic and Polymeric Materials, Tokyo Institute of Technology, 2-12-1-S8-24 Ookayama, Meguro-ku, Tokyo 152-8552, Japan

ABSTRACT: The fully π-conjugated donor–acceptor hybrid polymers Fl-TPA, Fl-TPA-TCNE, and Fl-TPA-TCNQ, which are composed of fluorene (Fl), triphenylamine (TPA), dimethylphenylamine, alkyne, alkyne-tetracyanoethylene (TCNE) adduct, and alkyne-7,7,8,8-tetracyanoquinodimethane (TCNQ) adduct, were synthesized. These polymers are completely amorphous in the solid film state and thermally stable up to 291–409 °C. Their molecular orbital levels and band gaps vary with their compositions. The TCNE and TCNQ units, despite their electron-acceptor characteristics, were found to enhance the π-conjugation lengths of Fl-TPA-TCNE and Fl-TPA-TCNQ (i.e., to produce red shifts in their absorption spectra and significant reductions in their band gaps). These changes are reflected in the electrical digital memory behavior of the polymers. Moreover, the TCNE and TCNQ units were found to diversify the digital memory modes and to widen the active polymer layer thickness window. In devices with aluminum top and bottom electrodes, the Fl-TPA polymer exhibits stable unipolar permanent memory behavior with high reliability. The Fl-TPA-TCNE and Fl-TPA-TCNQ devices exhibit stable unipolar permanent memory behavior as well as dynamic random access memory behavior with excellent reliability. These polymer devices were found to operate by either hole injection or hole injection along with electron injection, depending on the polymer composition. Overall, this study demonstrated that the incorporation of π-conjugated cyano moieties, which control both the π-conjugation length and electron-accepting power, is a sound approach for the design and synthesis of high-performance digital memory polymers. The TCNE and TCNQ polymers synthesized in this study are highly suitable active materials for the low-cost mass production of high-performance, polarity-free, programmable, volatile, and permanent memory devices that can be operated with very low power consumption, high ON/OFF current ratios, and high reliability.

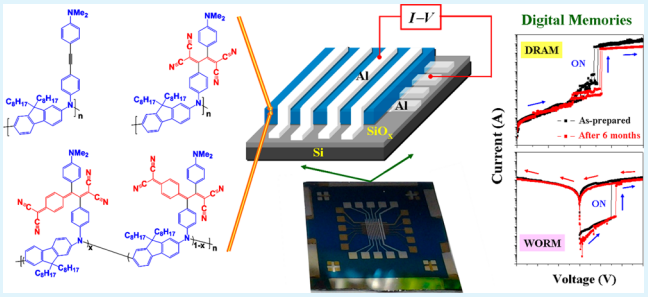

KEYWORDS: *π-conjugated donor–acceptor hybrid polymers, unipolar permanent digital memory, unipolar volatile digital memory, switching mechanism, charge trap and transport*

INTRODUCTION

Polymers containing aromatic amine or fluorene moieties have been investigated as hole-transporting materials for organic light emitting diodes (OLEDs) as well as p-type semiconductors for organic field effect transistors (OFETs) and organic solar cells.[1−27] These p-type polymers have recently been employed in memory devices that exhibit volatile and nonvolatile memory characteristics.[28−46] In contrast, organic molecules bearing cyano groups have been used as electron acceptors (i.e., n-type materials) in memory devices.[47−53] Therefore, it is interesting to mold these p- and n-type organic components into a single fully π-conjugated polymer system with the aim of enhancing and controlling device performance by adjusting the highest occupied and lowest unoccupied molecular orbital (HOMO and LUMO) levels and the band gap. Recently, the synthesis of such a π-conjugated aromatic amine and fluorene polymer was successfully demonstrated with Pd-catalyzed amination polymerization.[54] Furthermore, the side-chain alkynes of the π-conjugated aromatic amine and fluorene polymer were elegantly functionalized by performing [2 + 2] cycloaddition–-cycloreversion reactions with the cyano-containing molecules tetracyanoethylene (TCNE) and 7,7,8,8-tetracyanoquinodimethane (TCNQ) to produce fully π-conjugated donor–acceptor hybrid polymers.[54−57] The alkyne-acceptor (TCNE and TCNQ) addition reactions were found to proceed efficiently via click chemistry and to result in polymers with energy levels that are significantly lower because of the formation of strong acceptor moieties in the polymer

Received: March 5, 2014
Accepted: April 29, 2014
Published: April 29, 2014

   dx.doi.org/10.1021/am5013134 | ACS Appl. Mater. Interfaces 2014, 6, 8415–8425

repeat units. In other words, it has been confirmed that the controlled introduction of these organic acceptors into conjugated polymers is useful for the optimization of electronic states. Moreover, the polydispersities of the functionalized polymers are the same as those of the corresponding precursor polymer, which makes a quantitative comparison of their physical properties possible.

In this study, we investigated the digital memory characteristics of three π-conjugated donor−acceptor hybrid polymers: poly(4-((4-(dimethylamino)phenyl)ethynyl)phenylimino-9,9-dioctyl-fluorene-2,7-diyl) (Fl-TPA), poly(4-(1,1,4,4-tetracyano-3-(4-(dimethylamino)phenyl)-buta-1,3-dien-2-yl)phenylimino-9,9-dioctylfluor-ene-2,7-diyl) (Fl-TPA-TCNE), and poly(4-(1,1-dicyano-3-(4-(dicyanomethylene)cyclohexa-2,5-dien-1-ylidene)-3-(4-(dimethylamino)phenyl)-prop-1-en-2-yl)-phenylimino-9,9-diocytylfluorene-2,7-diyl-*ran*-4-(1,1-dicyano-3-(4-(dicyano-methylene)cyclohexa-2,5-dien-1-ylidene)-3-(4-(dimethylamino)phenyl)prop-1-en-2-yl)phenyl-imino-9,9-diocytylfluor-ene-2,7-diyl) (Fl-TPA-TCNQ) (Figure 1a). Memory devices were fabricated with the π-conjugated donor−acceptor hybrid polymers and top and bottom metal electrodes (Figure 1b). The active polymer layers were easily prepared through conventional solution coating and subsequent drying processes, and the bottom and top metal electrodes were prepared by performing electron-beam deposition and thermal evaporation in vacuum, respectively. The active polymer film layers were investigated by using synchrotron grazing incidence X-ray scattering (GIXS) and X-ray reflectivity (XR). In addition, the optical and electrochemical properties of the polymers were examined. The polymers exhibited excellent volatile and nonvolatile digital memory behavior that depended on the polymer system and the film layer thickness. Moreover, these devices were found to be p-type or p/n-type digital memory devices, depending on the polymer system.

EXPERIMENTAL SECTION

Fl-TPA was prepared by Pd-catalyzed polycondensation of 9,9-dioctyl-2,7-dibromofluorene and 4-((4-aminophenyl)ethynyl)-*N*,*N*-dimethylaniline in accordance with a synthetic method published in the literature.[54−57] To an ampule tube, 9,9-dioctyl-2,7-dibromofluorene (284 mg, 0.517 mmol), 4-((4-aminophenyl)ethynyl)-*N*,*N*-dimethylaniline (122 mg, 0.517 mmol), tris(dibenzylideneacetone)-dipalladium(0) ($Pd_2(dba)_3$, 13.3 mg, 0.0145 mmol), tri-*tert*-butylphosphine (P(*t*-Bu)$_3$, 22 μL, 0.088 mmol), sodium *tert*-butoxide (NaO*t*-Bu, 162 mg, 1.69 mmol), and toluene (0.60 mL) were added. The tube was attached to a vacuum line, sealed off, and then heated at 60 °C for 24 h. After cooling to room temperature, water was added, and the organic layer was extracted with dichloromethane (CH_2Cl_2). The solution was concentrated in vacuo and precipitated into methanol (MeOH, 300 mL), yielding a yellow powder. Reprecipitation from benzene into a mixture of MeOH and tetrahydrofuran (THF) (1:1, v/v; 1000 mL) was repeated until the monomer was removed. The obtained product was characterized by proton and carbon nuclear magnetic resonance (^{1}H and ^{13}C NMR) spectroscopy (JEOL AL300) and infrared (IR) spectroscopy (JASCO FT/IR-4100). Chemical shifts were recorded in ppm downfield from tetramethylsilane, using the solvent's residual signal as an internal reference. The resonance multiplicity is described as s (singlet), d (doublet), t (triplet), and m (multiplet). ^{1}H NMR (δ, 300 MHz, $CDCl_3$): 0.84−1.26 (m, 30n H), 1.83 (br s, 4n H), 2.98 (s, 6n H), 6.66 (d, J = 9 Hz, 2n H), 6.98−7.16 (m, 6n H), 7.34−7.51 (m, 6n H); ^{13}C NMR (δ, 75 MHz, $CDCl_3$): 14.14, 22.66, 23.98, 29.29, 29.41, 29.48, 30.07, 31.85, 40.26, 55.04, 87.58, 88.99, 110.65, 111.90, 115.32, 116.19, 119.59, 123.75, 127.09, 132.14, 132.48, 143.31, 149.84, 151.68, 152.04, 152.31; IR (ν, KBr): 2925, 2853, 2207, 1609, 1579, 1523, 1464, 1443, 1355, 1310, 1270, 1196, 1170, 1132, 946, 815, 525 cm^{-1}.

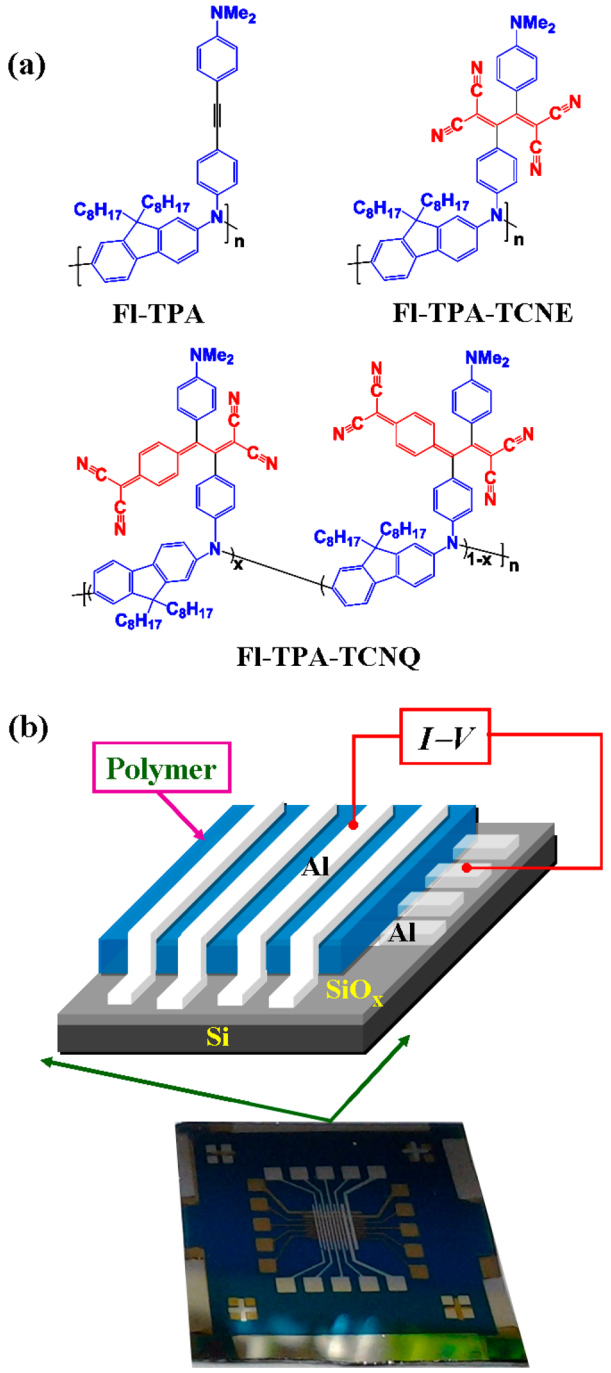

Figure 1. (a) Chemical structures of the model π-conjugated donor−acceptor hybrid polymers Fl-TPA, Fl-TPA-TCNE, and Fl-TPA-TCNQ. (b) Schematic diagram of a memory device cell; optical image of a memory device cell fabricated on a silicon substrate with a thermally grown oxide layer.

The weight-average molecular weight ($\overline{M_w}$) and polydispersity index (PDI) of Fl-TPA, determined by gel-permeation chromatography combined with multiangle light scattering (GPC-MALS), were 48 500 and 3.07, respectively. GPC measurements were carried out on a JASCO system (PU-980, CO-965, RI-930, UV-970, and AS-950) equipped with polystyrene gel columns using THF as an eluent at a flow rate of 1.0 mL/min after calibration with standard polystyrene, whereas absolute molecular weights were determined using a miniDAWN Tristar detector.[54−57]

Fl-TPA-TCNE and Fl-TPA-TCNQ were prepared by the reaction of Fl-TPA with TCNE and TCNQ, respectively, as described in the

literature.[54−57] To a solution of Fl-TPA (15 mg, 24 μmol) in 1,2-dichloroethane (3.0 mL), a TCNE solution in 1,2-dichloroethane (7.8 mM, 3.1 mL) was added. After the mixture was stirred at 20 °C for 5 min, the solvent was removed in vacuo. The obtained product was characterized by NMR spectroscopy with ^{1}H and ^{13}C probes and by IR spectroscopy. ^{1}H NMR (δ, 300 MHz, $CDCl_3$): 0.667 (br s, 3n H), 0.795 (t, J = 6 Hz, 3n H), 1.03−1.08 (m, 24n H), 1.57 (br s, 2n H), 1.85 (br s, 2n H), 3.15 (s, 6n H), 6.70 (d, J = 9 Hz, 2n H), 7.01 (d, J = 8 Hz, 2n H), 7.14 (d, J = 8 Hz, 2n H), 7.21 (s, 2n H), 7.62−7.68 (m, 4n H), 7.79 (d, J = 9 Hz, 2n H); ^{13}C NMR (δ, 75 MHz, $CDCl_3$): 14.17, 22.63, 24.10, 29.16, 29.36, 29.86, 31.74, 40.15, 55.48, 74.54, 77.23, 112.04, 112.75, 113.54, 113.82, 114.48, 118.68, 121.16, 122.88, 125.70, 131.87, 132.57, 138.94, 144.15, 152.92, 153.31, 164.66, 165.91; IR (ν, KBr): 2925, 2853, 2217, 1605, 1490, 1464, 1440, 1384, 1347, 1318, 1270, 1177, 945, 820, 671, 524 cm^{-1}.

To a solution of Fl-TPA (15 mg, 24 μmol) in 1,2-dichloroethane (30 mL) was added a TCNQ solution in 1,2-dichloroethane (1.5 m*M*, 16 mL). After the mixture was stirred at 80 °C for 24 h, the solvent was removed in vacuo. The obtained product was characterized by NMR spectroscopy with ^{1}H and ^{13}C probes and by IR spectroscopy. Note that some ^{13}C NMR peaks ascribed to the quaternary carbons were not clearly detected because of the random addition patterns of TCNQ. ^{1}H NMR (δ, 300 MHz, $CDCl_3$): 0.80−1.24 (m, 30n H), 1.77 (br s, 4n H), 2.95−3.13 (m, 6n H), 6.50−7.54 (m, 18n H); ^{13}C NMR (δ, 75 MHz, $CDCl_3$): 14.17, 22.65, 24.02, 29.28, 29.68, 29.98, 31.80, 40.19, 55.08, 111.10, 111.52, 112.38, 114.63, 114.93, 119.91, 124.16, 124.98, 127.48, 130.18, 130.33, 130.86, 130.99, 132.93, 134.58, 146.10, 152.04, 153.32; IR (ν, KBr): 2925, 2852, 2205, 1579, 1560, 1543, 1521, 1508, 1499, 1491, 1464, 1439, 1373, 1313, 1273, 1175, 942, 862, 819, 669 cm^{-1}.

Thermogravimetric analysis (TGA) was carried out on a Seiko SII TG/DTA 6200 at a heating rate of 10 °C/min between 20 and 600 °C. Differential scanning calorimetry (DSC) measurements were carried out on a Seiko SII DSC 6220 with a Seiko SII EXSTAR 6000 PC station.[54−57] The degradation temperature, $T_{d,5}$ (which caused 5% weight loss), and glass transition temperature, T_g, were 291 and 125 °C for Fl-TPA, 409 and 152 °C for Fl-TPA-TCNE, and 363 and 150 °C for Fl-TPA-TCNQ, respectively.

Each polymer was dissolved in chloroform and filtered through a PTFE membrane microfilter with a pore size of 0.2 μm, providing a 1.0 wt % solution. Polymer films were prepared on silicon substrates or bottom metal electrodes deposited on silicon substrates with a thick oxide layer by spin-coatings of the polymer solutions and subsequent drying at 40 °C in vacuum for 8 h. The film thicknesses were determined by using a spectroscopic ellipsometer (model M2000, Woollam).

Optical properties were measured in 1,2-dichloroethane using an ultraviolet−visible−near-infrared (UV−vis−NIR) spectrometer (JASCO model V-670). Cyclic voltammetry (CV) measurements were carried out in CH_2Cl_2 containing 0.1 M $(nC_4H_9)_4NClO_4$ at 20 °C under Ar using a classical three-electrode cell. The working, reference, and auxiliary electrodes were a glassy carbon disk electrode (0.07 cm^2), $Ag/Ag^+/CH_3CN/(nC_4H_9)_4NClO_4$, and a Pt wire, respectively. A scan rate of 100 mV/s was used. All potentials were referenced to the ferrocene/ferricinium (F_c/F_c^+) couple used as an internal standard.

GIXS analysis was carried out at the 4C1 and 4C2 beamlines of the Pohang Accelerator Laboratory (PAL) at Pohang University of Science & Technology according to a method described previously in the literature.[58−63] The polymer film samples, which were coated on silicon substrates, were measured using an X-ray radiation source with a 0.1380 nm wavelength and a 2D charge-coupled detector (2D CCD; MAR USA). The sample-to-detector distance was 2201.5 mm for grazing incidence small-angle X-ray scattering (GISAXS) measurements and 121.1 mm for grazing incidence wide-angle X-ray scattering (GIWAXS) measurements. The samples were mounted on a homemade z-axis goniometer equipped with a vacuum. The incident angle, α_i, of the X-ray beam was set at 0.160°, which is between the critical angles of the films and the Si substrate ($\alpha_{c,f}$ and $\alpha_{c,s}$, respectively). All GIXS measurements were carried out at 25 °C. Each measurement was collected for 60 s. Scattering angles were corrected according to the positions of the X-ray beams reflected from the silicon substrate with respect to a precalibrated silver behenate (TCI, Japan) powder. Aluminum foil pieces were applied as a semitransparent beam stop because the intensity of the specular reflection from the substrate was much stronger than the scattering intensity of the polymer films near the critical angle.

XR analysis was further conducted for the polymer samples at the 3C2 and 8C1 beamlines[64−66] of the PAL. Samples were mounted on a Huber four-circle goniometer equipped with a scintillation counter with an enhanced dynamic range (Bede Scientific, EDR) as a detector. The X-ray beam with a wavelength λ of 0.1541 nm was collimated at the sample position to 2.0 mm (horizontal) by 0.1 mm (vertical). Specular reflection was measured in $\theta - 2\theta$ scanning mode. The reflectivity R (i.e., the ratio of the reflected beam intensity to the primary beam intensity) was measured; here, the primary beam intensity was monitored with an ionization chamber.

Devices were fabricated as follows. Aluminum (Al) was deposited on silicon substrates with a thick oxide layer as bottom electrode strips (100−200 μm width) with a thickness of 300 nm by electron beam sputtering in vacuum through a shadow mask. Then polymer films were deposited onto the Al bottom electrodes by spin-coating the polymer solutions and subsequent drying at 40 °C in vacuum for 8 h. Thereafter, Al top electrode strips (100−200 μm width) were deposited with a thickness of 300 nm onto the polymer layers by thermal evaporation in vacuum through a shadow mask. The obtained device cells had sizes ranging from 100 × 100 to 200 × 200 μm^2. Current−voltage (I−V) measurements and stress tests of the device were carried out in ambient air using a Keithley 4200-SCS semiconductor characterization system. I−V curves were recorded by performing forward and reverse voltage scans between −10.0 and +10.0 V at a scan rate of 500 mV/s.

RESULTS AND DISCUSSION

The π-conjugated donor−acceptor hybrid polymers were investigated by performing UV−vis−NIR spectroscopy and CV analysis. The absorption maxima, λ_{max}, of these polymers are in the range 450−700 nm. As shown in Figure 2a−c, the cycloaddition−cycloreversions of TCNE and TCNQ produce significant red shifts in the spectra with respect to the absorption band of Fl-TPA because of the (4-aminophenyl)-ethynyl moiety. From the UV−vis−NIR spectra, the band gaps (i.e., the differences between the HOMO and LUMO levels of the polymers) were estimated to be 2.95 eV for Fl-TPA, 1.94 eV for Fl-TPA-TCNE, and 1.46 eV for Fl-TPA-TCNQ. The oxidation half-wave potentials ($E_{1/2}$) versus F_c/F_c^+ were determined to be 0.09 V for Fl-TPA, 0.34 V for Fl-TPA-TCNE, and 0.21 V for Fl-TPA-TCNQ (Figure 2d−f). By assuming that the HOMO level for the F_c/F_c^+ standard is −4.80 eV with respect to the zero vacuum level, the HOMO level of each polymer was estimated from the measured $E_{1/2}$ data. The LUMO level of each polymer was calculated from the obtained optical band gap and the HOMO level. The determined HOMO and LUMO levels were −4.89 and −1.94 eV for Fl-TPA, −5.14 and −3.20 eV for Fl-TPA-TCNE, and −5.01 and −3.55 eV for Fl-TPA-TCNQ, respectively. These results indicate that the cycloaddition−cycloreversions of TCNE and TCNQ lower the HOMO and LUMO levels of the resulting polymers. In particular, the insertions of TCNE and TCNQ reduce the LUMO level significantly and lower the band gap. These red shifts in the absorption as well as the reductions in the HOMO and LUMO levels and the band gaps are attributed to both the extensions of the π-conjugation lengths and the enhancements of intramolecular charge transfer that result from the insertions of TCNE and TCNQ, which override any

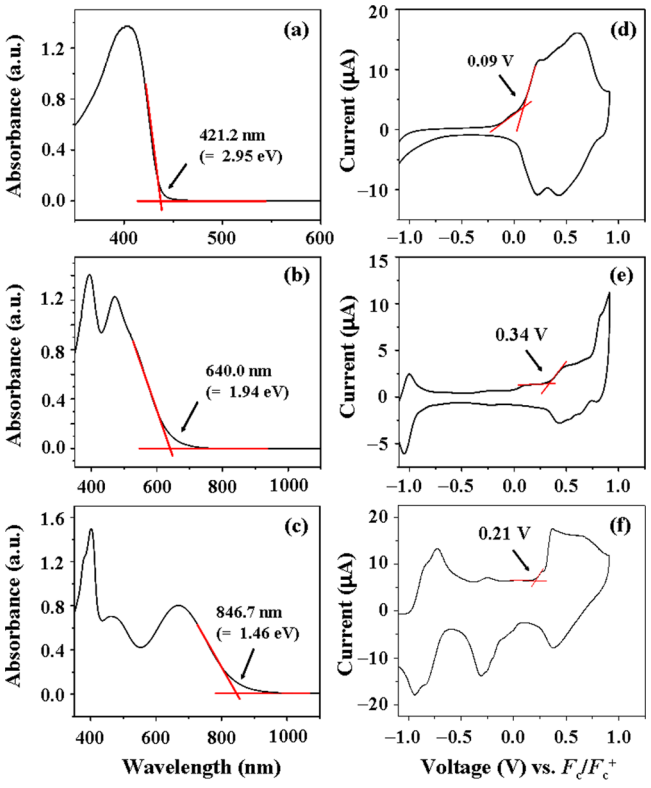

Figure 2. UV−vis−NIR spectra and CV responses of the polymers: (a, d) Fl-TPA, (b, e) Fl-TPA-TCNE, and (c, f) Fl-TPA-TCNQ. The UV−vis−NIR spectra (a−c) were measured in 1,2-dichloroethane. CV responses (d−f) were measured in CH_2Cl_2 containing 0.1 M $(nC_4H_9)_4NClO_4$ at 20 °C under Ar using a classical three-electrode cell. The working, reference, and auxiliary electrodes were a glassy carbon disk electrode (0.07 cm^2), $Ag/Ag^+/CH_3CN/(nC_4H_9)_4NClO_4$, and a Pt wire, respectively. A scan rate of 100 mV/s was used. All potentials were referenced to the ferrocene/ferricinium (F_c/F_c^+) couple used as an internal standard.

possible blue shifts because of the electron-accepting cyano groups.

The morphological structures of thin films (30−40 nm thick) of the polymers deposited on silicon substrates were investigated with synchrotron GISAXS and GIWAXS analyses. As shown in Figure 3a−c, all of the polymer films produce featureless GISAXS patterns, which indicates that no nanostructures are present in the polymer films. The polymer films also produce GIWAXS patterns that are featureless except for two amorphous ring scatterings (Figure 3d−f), which confirms that the polymer films are amorphous. For these polymer films, the ring scatterings in the low-angle region might originate from the mean interdistance of the polymer chains, whereas that in the high-angle region might be due to the mean interdistance of the side groups and/or that between the side groups and the polymer backbones. In particular, the scattering rings of the individual polymer films in the high-angle region are slightly anisotropic in intensity toward the meridian line, which indicates that the polymer chains are oriented somewhat preferentially in the film plane rather than randomly. The two scattering rings were determined to have *d*-spacings of 1.650 nm (4.8°) and 0.496 nm (16.0°) for the Fl-TPA film, 1.340 nm (5.9°) and 0.518 nm (15.3°) for the Fl-TPA-TCNE film, and 1.320 nm (6.0°) and 0.505 nm (15.7°) for the Fl-TPA-TCNQ film.

The polymer films were further investigated with synchrotron XR analysis; representative XR profiles are shown in Figure 4. The XR data were satisfactorily fitted using the Parratt algorithm.[67−69] The results of the analysis are summarized in Table 1. The electron densities, ρ_e, were 358.15 nm^3 for the Fl-TPA film, 390.07 nm^3 for the Fl-TPA-TCNE film, and 397.16 nm^3 for the Fl-TPA-TNCQ film. These results indicate that the electron densities of the Fl-TPA-TCNE and Fl-TPA-TNCQ films are significantly increased by the incorporation of TCNE and TCNQ in the repeat units. These ρ_e values were correlated with the *d*-spacing values (i.e., the interdistances of the polymer chains) determined in the GIWAXS analysis. The XR analysis found that the film surface roughnesses, σ, are 0.43 nm for the Fl-TPA film, 0.95 nm for the Fl-TPA-TCNE film, and 0.10 nm for the Fl-TPA-TCNQ film. These surface roughness results confirm that high-quality films of these polymers can be easily fabricated with conventional solution coating and subsequent drying processes.

Memory devices were fabricated with these polymers with various active layer thicknesses on silicon substrates with thermally grown oxide layers, as shown in Figure 1b; Al top and bottom electrodes were adopted in the fabrication of these devices. Representative measured *I*−*V* data are shown in Figures 5−7. All of the active polymer layers in the devices are initially in a high-resistance state, namely, the OFF state, regardless of the layer thickness. Furthermore, for all of the polymer devices with 40 nm thick layers, no sharp electrical transition is evident from the OFF state to a high-conductivity state (i.e., the ON state) when a negative or positive voltage is applied up to −8.0 or +8.0 V (Figures 5a,b, 6a,b, and 7a,b). The 30 nm thick Fl-TPA film layer also could not be switched to the ON state (Figure 5c,d). In contrast, the 30 nm thick Fl-TPA-TCNE film layer undergoes a sharp electrical transition from the OFF state to the ON state at −5.0 or +5.0 V (which corresponds to $V_{c,ON}$, the critical voltage to switch the device on) when a negative or positive voltage is applied from 0 to −8.0 or +8.0 V with a compliance current of 0.01 A (Figure 6c,d). This OFF-to-ON transition can function as a "writing" process. The ON state is retained when the electrical power is turned on. However, the active polymer layer in the ON state is returned to the OFF state by a reverse voltage sweep or when the power is turned off. This ON-to-OFF transition can function as an "erasing" process. The OFF state (i.e., the erased state) can again be switched to the ON state (i.e., a stored state) when a negative or positive voltage greater than the switching-ON threshold voltage is applied, which indicates that this memory device is rewritable. The ON/OFF current ratio was estimated to be in the range 10^4−10^5, depending on the reading voltage. Thus, the device with a 30 nm thick Fl-TPA-TCNE active layer demonstrates excellent dynamic random access memory (DRAM) behavior. Similar DRAM behavior was observed for the 30 nm thick Fl-TPA-TCNQ device (Figure 7c,d): $V_{c,ON} = \pm 3.2$ V and its ON/OFF ratio is in the range 10^4−10^5.

Surprisingly, the devices with 20 nm thick polymer layers were found to exhibit quite different memory behavior. As shown in Figure 5e,f, the Fl-TPA layer exhibits an abrupt increase in current at −3.1 or +3.0 V when a negative or positive voltage is applied. The ON state is retained even during reverse and forward voltage sweeps, and this is also the case even after the power is turned off. Moreover, the ON state could not be switched off by forward or reverse voltage sweeps with an even higher compliance current (0.10 A, which is 10

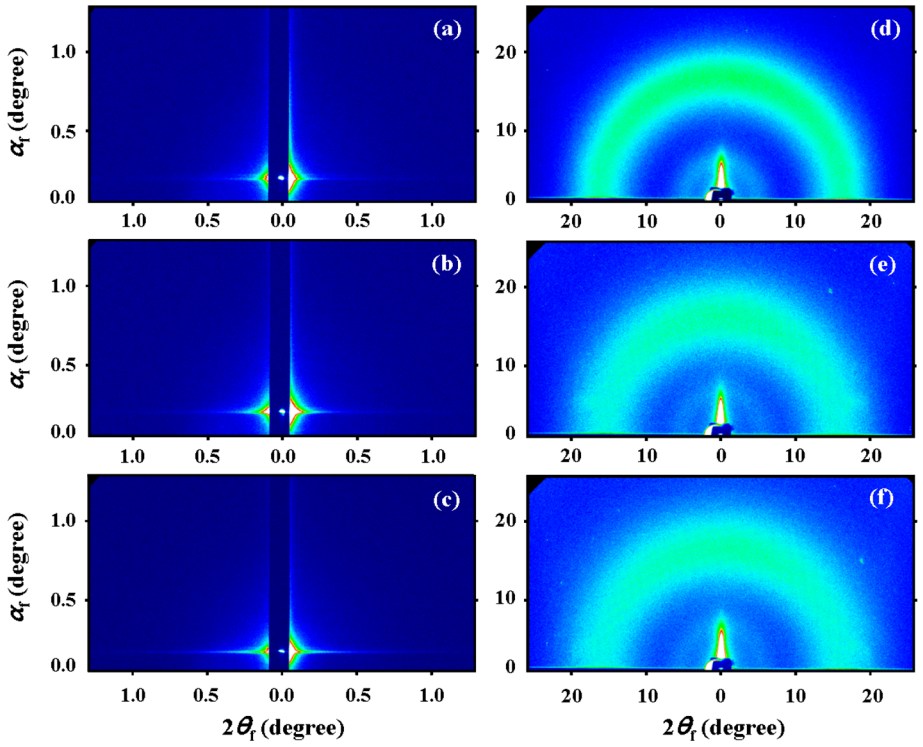

Figure 3. Representative synchrotron GIXS patterns of the polymer films (30−40 nm thick) coated onto silicon substrates: (a) GISAXS and (d) GIWAXS patterns of Fl-TPA, (b) GISAXS and (e) GIWAXS patterns of Fl-TPA-TCNE, and (c) GISAXS and (f) GIWAXS patterns of Fl-TPA-TCNQ. The wavelength, λ, of the X-ray beam was 0.1380 nm; the incident angle, α_i, of the X-ray beam was set at 0.160°.

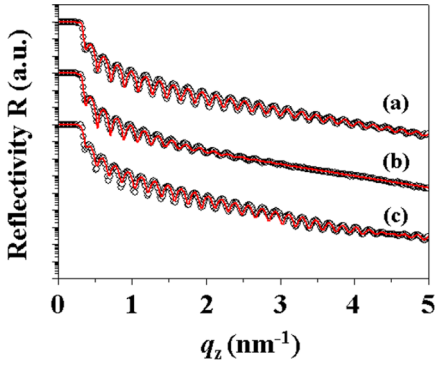

Figure 4. Representative XR profiles of the polymer films (30−40 nm thick) coated onto silicon substrates: (a) Fl-TPA, (b) Fl-TPA-TCNE, and (c) Fl-TPA-TCNQ. The wavelength, λ, of the X-ray beam was 0.1541 nm. The symbols are the measured data, and the solid lines are the curves fitted to the data by assuming homogeneous electron density distributions within the films.

times higher than the compliance current in the first sweep that switches the device on). These results show that the device with a 20 nm thick Fl-TPA layer exhibits excellent write-once read-many times (WORM) memory characteristics. The ON/OFF ratio was found to be in the range 10^4−10^5, depending on the read voltage. Similar WORM memory behavior was observed for the devices with 20 nm thick Fl-TPA-TCNE and Fl-TPA-TCNQ layers (Figures 6e,f and 7e,f). The $V_{c,ON}$ values were found to be −4.2 or +4.7 V for the Fl-TPA-TCNE device and −3.0 or +3.7 V for the Fl-TPA-TCNQ device. Similar WORM memory behavior was observed for all of the devices with 10 nm thick polymer films (Figures 5g,h, 6g,h, and 7g,h). The $V_{c,ON}$ values were found to be −2.7 or +2.0 V for the Fl-TPA device, ±3.7 for the Fl-TPA-TCNE device, and ±1.2 V for the Fl-TPA-TCNQ device.

Overall, the π-conjugated hybrid polymers exhibit both composition- and thickness-dependent memory characteristics. Fl-TPA polymer films exhibit only unipolar WORM memory (i.e., permanent memory) behavior within a narrow thickness window, 10−20 nm. The additions of TCNE and TCNQ to the Fl-TPA polymer enlarge the film thickness window (which can reveal memory behavior) to the range 10−30 nm and add an additional memory function, unipolar DRAM, to the unipolar permanent memory behavior. Interestingly, the contributions of the incorporated TCNE and TCNQ units to the memory

Table 1. Structural Parameters of the Polymer Films Deposited on Silicon Substrates with Native Oxide Layers[a]

	Si substrate			polymer layer			SiO_2 interlayer		
sample (polymer/Si)	d (nm)[b]	ρ_e (nm^{-3})[c]	σ (nm)[d]	d (nm)[b]	ρ_e (nm^{-3})[c]	σ (nm)[d]	d (nm)[b]	ρ_e (nm^{-3})[c]	σ (nm)[d]
Fl-TPA		746.09	0.35	32.2	358.15	0.43	0.73	697.16	0.16
Fl-TPA-TCNE		717.73	0.39	32.8	390.07	0.95	0.43	669.85	0.25
Fl-TPA-TCNQ		739.71	0.30	33.8	397.16	0.10	1.20	678.36	0.33

[a]Determined with synchrotron XR analysis. [b]Layer thickness. [c]Electron density of layer. [d]Roughness of layer in contact with air, the lower layer, or the upper layer.

dx.doi.org/10.1021/am5013134 | ACS Appl. Mater. Interfaces 2014, 6, 8415−8425

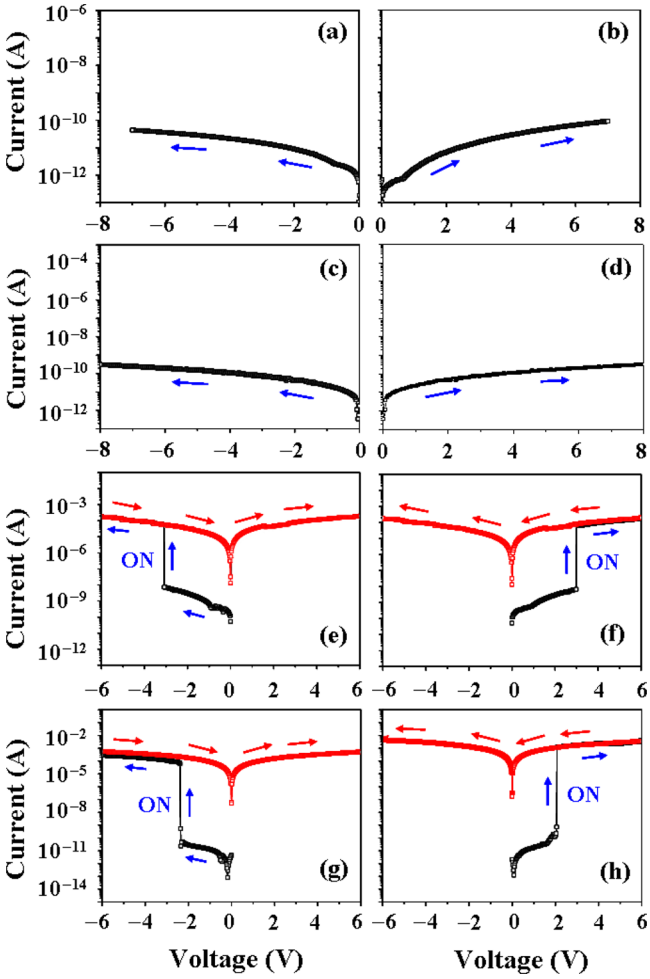

Figure 5. Typical $I-V$ curves of the Al/Fl-TPA/Al devices, which were measured with a compliance current set of 0.01 A: (a, b) 40 nm thick films, (c, d) 30 nm thick films, (e, f) 20 nm thick films, and (g, h) 10 nm thick films. The electrode contact area was 100 × 100 μm^2.

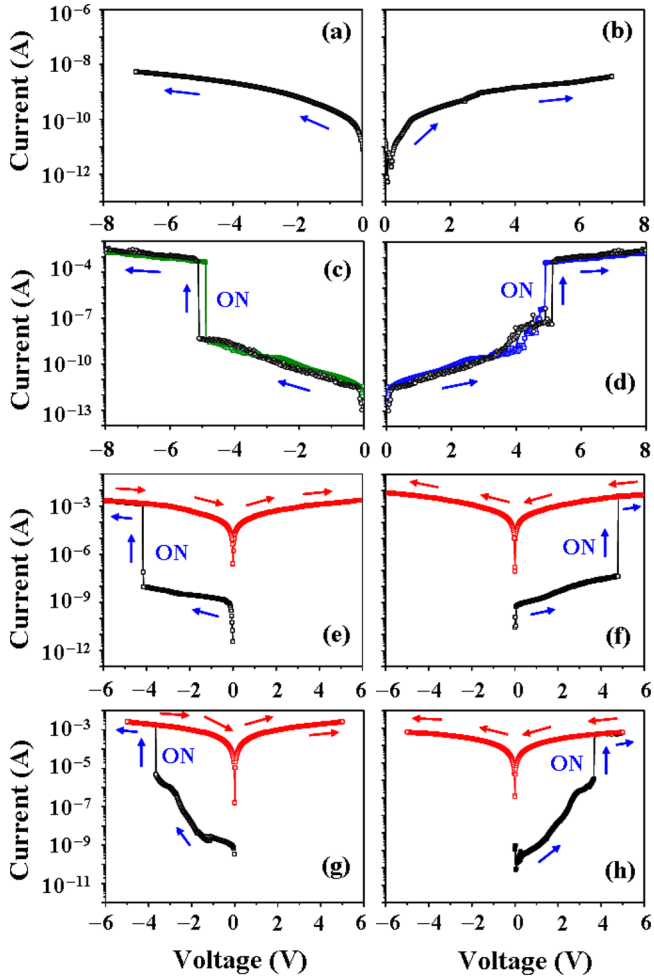

Figure 6. Typical $I-V$ curves of the Al/Fl-TPA-TCNE/Al devices, which were measured with a compliance current set of 0.01 A: (a, b) 40 nm thick films, (c, d) 30 nm thick films, (e, f) 20 nm thick films, and (g, h) 10 nm thick films. The electrode contact area was 100 × 100 μm^2.

performances are somewhat different. The addition of TCNE was found to produce an increase in the $V_{c,ON}$ value. In contrast, the addition of TCNQ produces a lowering of the $V_{c,ON}$ level.

For the polymer devices, the stabilities of the ON and OFF states were further examined at room temperature under ambient air conditions by using reading voltages of +1.0 or −2.0 V (for the ON state) and +1.0 or −1.0 V (for the OFF state). The results are displayed in Figures 8 and 9. Once the unipolar Fl-TPA-TCNE device with DRAM behavior is switched to the ON state by applying +6.0 V at a compliance current of 0.01 A, this state is well-retained without any degradation for a test period of 1.0×10^9 s (Figure 8b). When the device in the ON state is switched off by turning the power off, the OFF state is also well-retained without any degradation for a test period of 1.0×10^9 s (Figure 8b). Similar stability results were observed for the ON and OFF states of the unipolar Fl-TPA-TCNQ device with DRAM behavior (Figure 8c). All of the ON and OFF states of the devices with WORM memory behavior were found to exhibit excellent stabilities without any degradation for a test period of 4.0×10^4 s (Figure 9). Moreover, it was confirmed that all of the polymer devices in both the unipolar DRAM and WORM memory modes still function properly after being kept under ambient air conditions for 6 months (Figure 10).

Overall, the memory devices fabricated with Fl-TPA, Fl-TPA-TCNE, and Fl-TPA-TCNQ were found to exhibit excellent unipolar volatile and nonvolatile memory performance as well as excellent reliability.

The $I-V$ data were further analyzed in detail with various conduction models[70−73] in order to investigate the electrical switching characteristics and current conduction mechanisms of the polymer films in the devices. As shown in Figure 11, the $I-V$ data for the OFF state can be satisfactorily fitted with the trap-limited space charge limited conduction (SCLC) model, and those for the ON state can be satisfactorily fitted with the ohmic conduction model. These results suggest that under electrical fields all of the polymer film layers in the OFF state are governed by the SCLC conduction mechanism and that their ON states are governed by the ohmic conduction mechanism. Moreover, the current levels of the devices in the ON state were found to be independent of the device cell sizes, which is indicative of heterogeneously localized filament formation in the polymer film layers in the ON state. These results show that the excellent volatile and nonvolatile memory behaviors of the Fl-TPA, Fl-TPA-TCNE, and Fl-TPA-TCNQ

dx.doi.org/10.1021/am5013134 | ACS Appl. Mater. Interfaces 2014, 6, 8415−8425

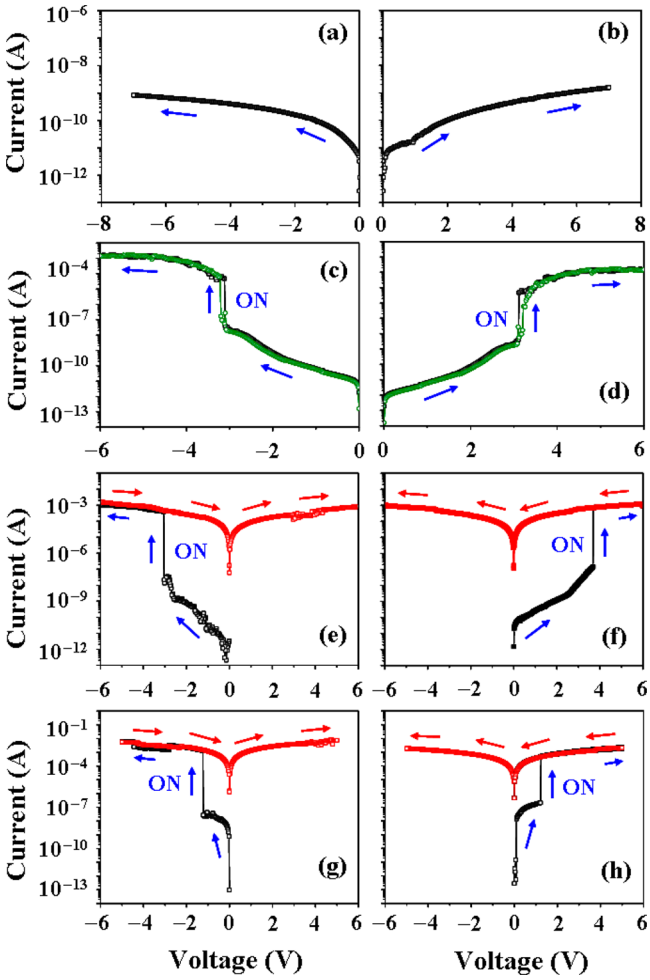

Figure 7. Typical $I-V$ curves of the Al/Fl-TPA-TCNQ/Al devices, which were measured with a compliance current set of 0.01 A: (a, b) 40 nm thick films, (c, d) 30 nm thick films, (e, f) 20 nm thick films, and (g, h) 10 nm thick films. The electrode contact area was 100 × 100 μm^2.

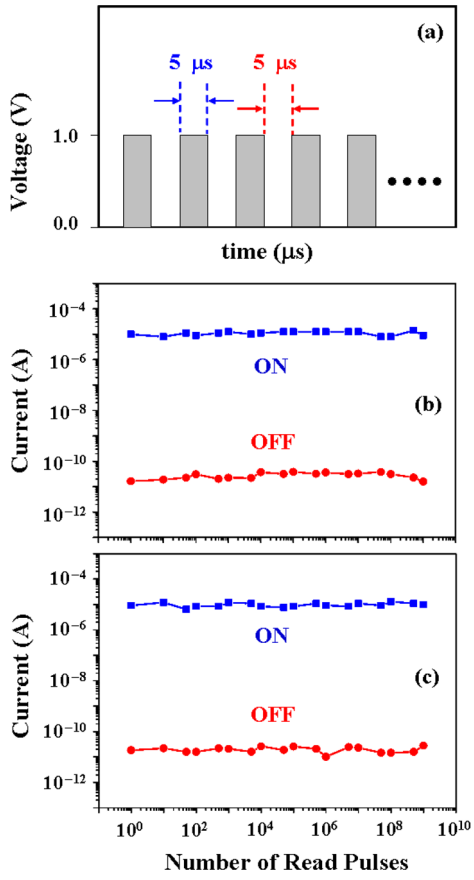

Figure 8. Long time responses (i.e., retention times) of the ON and OFF states of the polymer devices with DRAM behavior: (a) reading of +1.0 V in pulse mode, which was in the measurements, (b) Al/Fl-TPA-TCNE(30 nm thick)/Al, and (c) Al/Fl-TPA-TCNQ(30 nm thick)/Al. All measurements were carried out under ambient air conditions.

films are governed by trap-limited SCLC and local filament formation.

For the Fl-TPA devices, the energy barrier (0.61 eV) to hole injection from the Al electrode (Φ(work function) = −4.28 eV) into the HOMO level is lower than that (2.34 eV) for electron injection from the Al electrode into the LUMO level and thus the conduction process in these devices is dominated by hole injection. A similar hole injection-driven conduction process is favorable for the Fl-TPA-TCNE devices. However, the energy barrier (0.86 eV) for the hole injection process is higher for the Fl-TPA-TCNE devices than for the Fl-TPA devices. This relatively high energy barrier could contribute to the increase in the $V_{c,ON}$ values. Interestingly, the energy barriers (0.73 eV) to hole and electron injections from the electrodes in the Fl-TPA-TCNQ devices are the same. Thus, the Fl-TPA-TCNQ devices possibly undergo conduction processes governed by both hole and electron injection. Furthermore, the low $V_{c,ON}$ values of these devices might be due, in part, to such cooperative hole and electron injection.

Charge-trapping sites might arise because of the chemical compositions of the polymer chains. The hybridized fluorene and triphenylamine units as well as the dimethylphenylamine group are all electron donors that can act as nucleophilic sites, whereas the alkyne-TCNE and alkyne-TCNQ adduct units as well as the ethynylene linker are electron acceptors that can act as electrophilic sites. When a voltage is applied to the polymer layer in the device, the nucleophilic units enriched with holes become hole-trapping sites, whereas the electrophilic groups enriched with electrons act as electron-trapping sites. Considering the induction and resonance effects of the chemical components and mole fractions, the hybridized fluorene and triphenylamine units and the dimethylphenylamine groups of Fl-TPA and Fl-TPA-TCNE are expected to have higher charge trap and stabilization abilities than the other groups. In the case of Fl-TPA-TCNQ, these electron-donor moieties are expected to have charge trap and stabilization abilities comparable to those of the alkyne-TCNQ adduct unit. Thus, the nucleophilic and electrophilic groups are likely to act as charge-trapping sites and further to serve as stepping stones that enable the flow of charge carriers. When the applied bias reaches $V_{c,ON}$ or higher, the flow of charge carriers (i.e., current) takes place favorably via hopping processes through the charge-trapping sites as stepping stones (i.e., local filament formation), which have a mean interdistance of 1.320−1.650 nm or less. However, the polymers showed thickness-dependent memory characteristics, as discussed above. The results indicate that such electrical switching and charge carrier flows can be limited to the polymer film layers with a thickness of 20−30 nm or less. These switching behaviors might be

dx.doi.org/10.1021/am5013134 | ACS Appl. Mater. Interfaces 2014, 6, 8415−8425

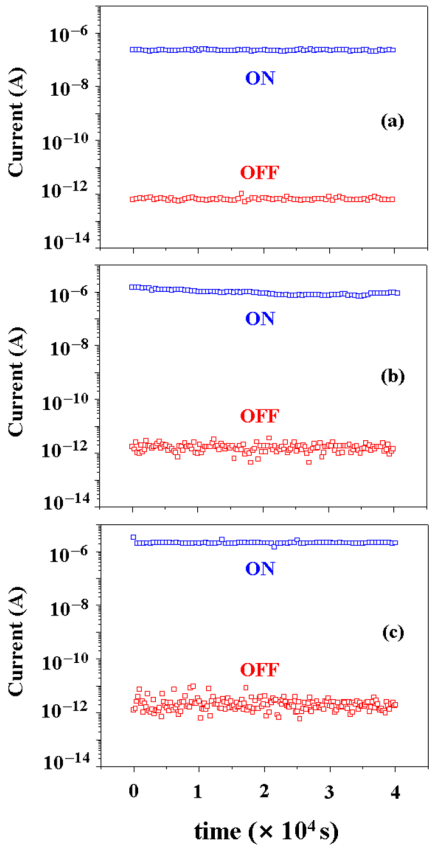

Figure 9. Long time responses (i.e., retention times) of the ON and OFF states of the Al/polymer(20 nm thick)/Al devices with WORM memory behavior to reading voltages of +1.0 V in pulse mode for (a) Fl-TPA, (b) Fl-TPA-TCNE, and (c) Fl-TPA-TCNQ. All measurements were carried out under ambient air conditions.

attributed to the nucleophilic and electrophilic groups in the polymers that may have a limited ability to trap charges and stabilize the trapped charges and a limited performance in serving as stepping stones for the hopping process of charge carriers.

CONCLUSIONS

In this study, three π-conjugated donor−acceptor hybrid polymers (Fl-TPA, Fl-TPA-TCNE, and Fl-TPA-TCNQ), which are composed of fluorene (Fl), triphenylamine (TPA), dimethylphenylamine, alkyne, alkyne-TCNE adduct, and alkyne-TCNQ adduct, were investigated. The polymers are thermally stable up to 291−409 °C. All of the polymer thin films are amorphous. Despite their electron-acceptor characteristics, the additions of TCNE and TCNQ to the side-chain alkynes of Fl-TPA extend the π-conjugation length and enhance the intramolecular charge transfer, which result in red shifts rather than blue shifts in the UV−vis absorption spectra. These transformation reactions also decrease the HOMO and LUMO levels as well as narrow the band gaps. The changes in the molecular orbitals and band gaps were found to be directly related to the electrical digital memory behavior. In devices with Al top and bottom electrodes, the Fl-TPA polymer exhibits stable unipolar permanent memory behavior over only a narrow film thickness window of 10−20 nm, which is dominated by hole injection processes. However, this electrical memory behavior is altered by the incorporation of the TCNE and TCNQ units. In addition to unipolar permanent memory

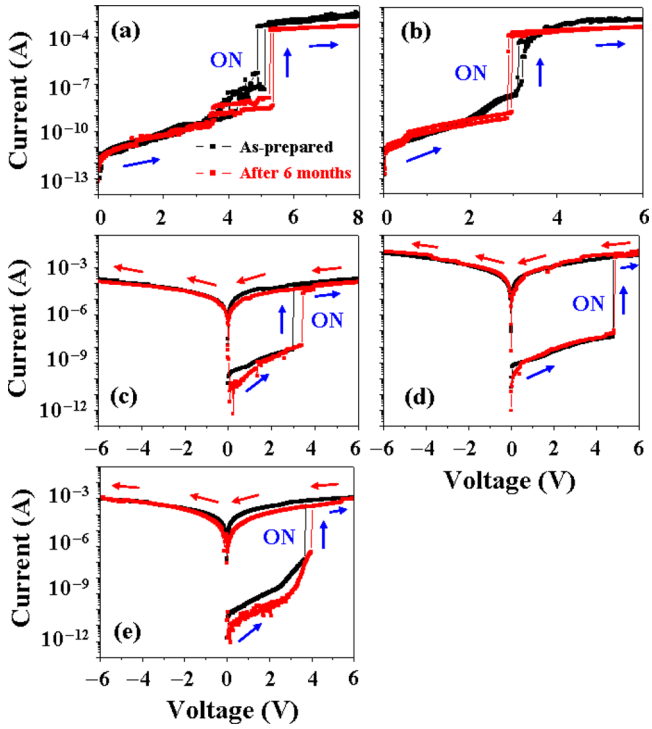

Figure 10. Reliability of the Al/polymer/Al devices: (a) Fl-TPA-TCNE (30 nm thick), (b) Fl-TPA-TCNQ (30 nm thick), (c) Fl-TPA (20 nm thick), (d) Fl-TPA-TCNE (20 nm thick), and (e) Fl-TPA-TCNQ (20 nm thick). In the reliability tests, the devices were stored under ambient air conditions for 6 months. The electrode contact area was 100 × 100 μm^2.

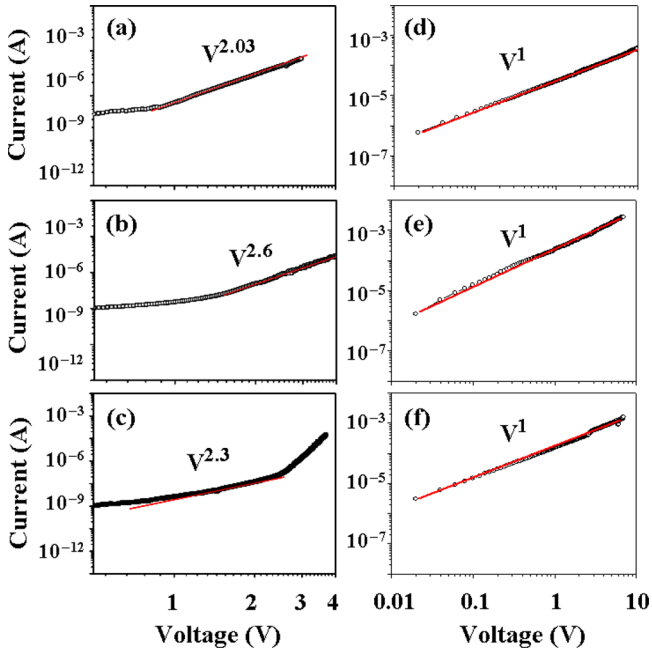

Figure 11. *I*−*V* plots of the Al/polymer (20 nm thick)/Al devices. The OFF state: (a) Fl-TPA, (b) Fl-TPA-TCNE, and (c) Fl-TPA-TCNQ. The symbols are the measured data, and the solid lines are curves fitted with the trap-limited space charge limited current (SCLC) model. The ON state: (d) Fl-TPA, (e) Fl-TPA-TCNE, and (f) Fl-TPA-TCNQ. The symbols are the measured data, and the solid lines are curves fitted with the ohmic current model.

dx.doi.org/10.1021/am5013134 | ACS Appl. Mater. Interfaces 2014, 6, 8415−8425

behavior, the Fl-TPA-TCNE polymer exhibits stable unipolar volatile memory behavior over a slightly wider thickness window of 10−30 nm at slightly higher operation voltages. However, these memory behaviors were still found to be dominated by hole injection processes. Such memory characteristics might result from the positive contribution of the extension of the π-conjugation length, which can override any negative contribution to the hole injection process because of the electron-accepting TCNE units. Similar volatile and nonvolatile memory behaviors and operation thickness window were observed for the Fl-TPA-TCNQ polymer. However, its memory behavior was found to be driven by both hole and electron injection processes, in which the electron donor and acceptor moieties cooperatively work together as charge-trapping sites. These cooperative charge injection processes mean that the memory devices can be operated at relatively low voltages. Finally, all of the volatile and nonvolatile memory behaviors of these polymers were found to be governed by trap-limited SCLC and local filament formation. Overall, this study has demonstrated that the incorporation of π-conjugated cyano moieties (which can control the π-conjugation length and the electron-accepting ability) is a sound approach for the design and synthesis of high-performance digital memory polymers. The polymers containing TCNE and TCNQ (Fl-TPA-TCNE and Fl-TPA-TCNQ, respectively) are highly active materials suitable for the low-cost mass production of high-performance, polarity-free, programmable, volatile, and permanent memory devices that can be operated with very low power consumption, high ON/OFF current ratios, and high reliability.

AUTHOR INFORMATION

Corresponding Authors

* (T.M.) Tel: +81-3-5734-3774; Fax: +81-3-5734-3774; E-mail: michinobu.t.aa@m.titech.ac.jp.

*(M.R.) Tel: +82-54-279-2120; Fax: +82-54-279-3399; E-mail: ree@postech.edu.

Author Contributions

§Y.-G.K. and D.M.K. contributed equally to this work.

Notes

The authors declare no competing financial interest.

ACKNOWLEDGMENTS

This study was supported by the National Research Foundation (NRF) of Korea (Doyak Program 2011-0028678 and Center for Electro-Photo Behaviors in Advanced Molecular Systems (2010-0001784)) and the Ministry of Science, ICT and Future Planning (MSIP) and the Ministry of Education (BK21 Plus Program and Global Excel Program). This work was also supported by the Ministry of Education, Culture, Sports, Science and Technology (MEXT), Japan (Grant-in-Aid for Scientific Research (A), no. 22685023). The synchrotron X-ray scattering measurements at the Pohang Accelerator Laboratory were supported by the MSIP, POSTECH Foundation, and POSCO Company.

REFERENCES

(1) Blouin, N.; Michaud, A.; Gendron, D.; Wakim, S.; Blair, E.; Neagu-Plesu, R.; Belletête, M.; Durocher, G.; Tao, Y.; Leclerc, M. Toward a Rational Design of Poly(2,7-carbazole) Derivatives for Solar Cells. *J. Am. Chem. Soc.* **2008**, *130*, 732−742.

(2) Michinobu, T.; Kumazawa, H.; Shigehara, K. Nitrogen-Linked Aromatic Poly(2,7-carbazole)s: Partially Annulated Poly(m-aniline)s. *Chem. Lett.* **2007**, *36*, 620−621.

(3) Michinobu, T.; Kumazawa, H.; Otsuki, E.; Usui, H.; Shigehara, K. Synthesis and Properties of Nitrogen-Linked Poly(2,7-carbazole)s as Hole-Transport Material for Organic Light Emitting Diodes. *J. Polym. Sci., Part A: Polym. Chem.* **2009**, *47*, 3880−3891.

(4) Beaupré, S.; Boudreault, P.-L. T.; Leclerc, M. Solar-Energy Production and Energy-Efficient Lighting: Photovoltaic Devices and White-Light-Emitting Diodes Using Poly(2,7-fluorene), Poly(2,7-carbazole), and Poly(2,7-dibenzosilole) Derivatives. *Adv. Mater.* **2010**, *22*, E6−E27.

(5) Friend, R. H.; Gymer, R. W.; Holmes, A. B.; Burroughes, J. H.; Marks, R. N.; Taliani, C.; Bradley, D. D. C.; Dos Santos, D. A.; Brédas, J. L.; Lögdlund, M.; Salaneck, W. R. Electroluminescence in Conjugated Polymers. *Nature* **1999**, *397*, 121−128.

(6) Wu, W.-C.; Chen, C.-Y.; Tian, Y.; Jang, S.-H.; Hong, Y.; Liu, Y.; Hu, R.; Tang, B. Z.; Lee, Y.-T.; Chen, C.-T.; Chen, W.-C.; Jen, A. K.-Y. Enhancement of Aggregation-Induced Emission in Dye-Encapsulating Polymeric Micelles for Bioimaging. *Adv. Funct. Mater.* **2010**, *20*, 1413−1423.

(7) Liu, Q.; Qu, Y.; Geng, Y.; Wang, F. Macromonomer Approach toward Fluorene-Based Monodisperse Conjugated Polymers. *Macromolecules* **2008**, *41*, 5964−5966.

(8) Tang, S.; Liu, M.; Lu, P.; Cheng, G.; Zeng, M.; Xie, Z.; Xu, H.; Wang, H.; Yang, B.; Ma, Y.; Yan, D. Fluorene Trimers with Various 9,9′-Substituents: The Synthesis, Characteristics, Condensed State Structures, and Electroluminescence Properties. *Org. Electron.* **2008**, *9*, 241−252.

(9) Jiang, H. J.; Wang, H. Y.; Feng, J. C.; Wang, C. M.; Fan, Q. L.; Wei, W.; Huang, W. Novel Oligomers Based on Fluorene and 2,4-Difluorobenzene: Correlation between the Structures and Optical Properties. *J. Polym. Sci., Part A: Polym. Chem.* **2006**, *44*, 4346−4353.

(10) Chi, C.; Wegner, G. Chain-Length Dependence of the Electrochemical Properties of Conjugated Oligofluorenes. *Macromol. Rapid Commun.* **2005**, *26*, 1532−1537.

(11) Geng, Y.; Trajkovska, A.; Katsis, D.; Ou, J. J.; Culligan, S. W.; Chen, S. H. Synthesis, Characterization, and Optical Properties of Monodisperse Chiral Oligofluorenes. *J. Am. Chem. Soc.* **2002**, *124*, 8337−8347.

(12) Scherf, U.; List, E. J. W. Semiconducting Polyfluorenes—Towards Reliable Structure−Property Relationships. *Adv. Mater.* **2002**, *14*, 477−487.

(13) Ranger, M.; Rondeau, D.; Leclerc, M. New Well-Defined Poly(2,7-fluorene) Derivatives: Photoluminescence and Base Doping. *Macromolecules* **1997**, *30*, 7686−7691.

(14) Boiteau, L.; Moroni, M.; Hilberer, A.; Werts, M.; de Boer, B.; Hadziioannou, G. Synthesis of a Diblock Copolymer with Pendent Luminescent and Charge Transport Units through Nitroxide-Mediated Free Radical Polymerization. *Macromolecules* **2002**, *35*, 1543−1548.

(15) Behl, M.; Zentel, R. Block Copolymers Build-Up of Electron and Hole Transport Materials. *Macromol. Chem. Phys.* **2004**, *205*, 1633−1643.

(16) Melucci, M.; Barbarella, G.; Zambianchi, M.; Benzi, M.; Biscarini, F.; Cavalline, M.; Bongini, A.; Fabbroni, S.; Mazzeo, M.; Anni, M.; Gigli, G. Poly(α-vinyl-ω-alkyloligothiophene) Side-Chain Polymers. Synthesis, Fluorescence, and Morphology. *Macromolecules* **2004**, *37*, 5692−5702.

(17) Tian, Y.; Chen, C. Y.; Haller, M. A.; Tucker, N. M.; Ka, J. W.; Luo, J.; Huang, S.; Jen, A. K. Y. Nanostructured Functional Block Copolymers for Electrooptic Devices. *Macromolecules* **2007**, *40*, 97−104.

(18) Lee, K. W.; Lin, H. C. Synthesis and Characterization of Liquid Crystalline Side-Chain Block Copolymers Containing Luminescent 4,4′-Bis(biphenyl)fluorene Pendants. *J. Polym. Sci., Part A: Polym. Chem.* **2007**, *45*, 4564−4572.

(19) Neher, D. Polyfluorene Homopolymers: Conjugated Liquid-Crystalline Polymers for Bright Blue Emission and Polarized Electroluminescence. *Macromol. Rapid Commun.* **2001**, *22*, 1365−1385.

(20) Gross, M.; Muller, D. C.; Nothofer, H.-G.; Scherf, U.; Neher, D.; Brauchle, C.; Meerholz, K. Improving the Performance of Doped π-Conjugated Polymers for Use in Organic Light-Emitting Diodes. *Nature* **2000**, *405*, 661−665.
(21) Suzuki, M.; Tokito, S.; Sato, F.; Igarashi, T.; Kondo, K.; Koyama, T.; Yamaguchi, T. Highly Efficient Polymer Light-Emitting Devices Using Ambipolar Phosphorescent Polymers. *Appl. Phys. Lett.* **2005**, *86*, 103507-1−103507-3.
(22) Deng, L.; Furuta, P. T.; Garon, S.; Li, J.; Kavulak, D.; Thompson, M. E.; Fréchet, J. M. J. Living Radical Polymerization of Bipolar Transport Materials for Highly Efficient Light Emitting Diodes. *Chem. Mater.* **2006**, *18*, 386−395.
(23) Sommer, M.; Lindner, S. M.; Thelakkat, M. Microphase-Separated Donor−Acceptor Diblock Copolymers: Influence of HOMO Energy Levels and Morphology on Polymer Solar Cells. *Adv. Funct. Mater.* **2007**, *17*, 1493−1500.
(24) Ma, B.; Kim, B. J.; Deng, L.; Poulsen, D. A.; Thompson, M. E.; Fréchet, J. M. J. Bipolar Copolymers as Host for Electroluminescent Devices: Effects of Molecular Structure on Film Morphology and Device Performance. *Macromolecules* **2007**, *40*, 8156−8161.
(25) Yeh, K. M.; Chen, Y. Vinyl Copolymers Containing Pendant 1,3,4-Oxadiazole Chromophores: Preparation and Electrochemical and Electroluminescent Properties. *J. Polym. Sci., Part A: Polym. Chem.* **2007**, *45*, 2259−2272.
(26) Sugiyama, K.; Hirao, A.; Hsu, J.-C.; Tung, Y.-C.; Chen, W.-C. Living Anionic Polymerization of Styrene Derivatives Para-Substituted with π-Conjugated Oligo(fluorene) Moieties. *Macromolecules* **2009**, *42*, 4053−4062.
(27) Li, C.; Hsu, J.-C.; Sugiyama, K.; Hirao, A.; Chen, W.-C.; Mezzenga, R. Synthesis and Self-Assembly Behavior of Poly-(fluorenylstyrene)-block-poly(2-vinylpyridine) Block Copolymers and Their Blends with Single Wall Carbon Nanotubes (SWCNTs). *Macromolecules* **2009**, *42*, 5793−5801.
(28) Ling, Q.-D.; Chang, F.-C.; Song, Y.; Zhu, C.-X.; Liaw, D.-J.; Chan, D. S.-H.; Kang, E.-T.; Neoh, K.-G. Synthesis and Dynamic Random Access Memory Behavior of a Functional Polyimide. *J. Am. Chem. Soc.* **2006**, *128*, 8732−8733.
(29) Liu, G.; Ling, Q.-D.; Kang, E.-T.; Neoh, K.-G.; Liaw, D.-J.; Chang, F.-C.; Zhu, C.-X.; Chan, S.-H. Bistable Electrical Switching and Write-Once Read-Many-Times Memory Effect in a Donor-Acceptor Containing Polyfluorene Derivative and Its Carbon Nanotube Composites. *J. Appl. Phys.* **2007**, *102*, 024502-1−024502-8.
(30) Kim, M.; Choi, S.; Ree, M.; Kim, O. Current-Dependent Switching Characteristics of PI-Diphenyl Carbamyl Films. *IEEE Electron Device Lett.* **2007**, *28*, 967−969.
(31) Hahm, S. G.; Choi, S.; Hong, S.-H.; Lee, T. J.; Park, S.; Kim, D. M.; Kim, J. C.; Kwon, W.; Kim, K.; Kim, M.-J.; Kim, O.; Ree, M. Electrically Bistable Nonvolatile Switching Devices Fabricated with a High Performance Polyimide Bearing Diphenylcarbamyl Moieties. *J. Mater. Chem.* **2009**, *19*, 2207−2214.
(32) Kim, D. M.; Park, S.; Lee, T. J.; Hahm, S. G.; Kim, K.; Kim, J. C.; Kwon, W.; Ree, M. Programmable Permanent Data Storage Characteristics of Nanoscale Thin Films of a Thermally Stable Aromatic Polyimide. *Langmuir* **2009**, *25*, 11713−11719.
(33) Kim, K.; Park, S.; Hahm, S. G.; Lee, T. J.; Kim, D. M.; Kim, J. C.; Kwon, W.; Ko, Y. G.; Ree, M. Nonvolatile Unipolar and Bipolar Bistable Memory Characteristics of a High Temperature Polyimide Bearing Diphenylaminobenzylidenylimine Moieties. *J. Phys. Chem. B* **2009**, *113*, 9143−9150.
(34) Lee, T. J.; Chang, C.-W.; Hahm, S. G.; Kim, K.; Park, S.; Kim, D. M.; Kim, J.; Kwon, W.-S.; Liou, G.-S.; Ree, M. Programmable, Digital Memory Devices Based on Nanoscale Thin Films of a Thermally, Dimensionally Stable Polyimide. *Nanotechnology* **2009**, *20*, 135204.
(35) Lee, T. J.; Park, S.; Hahm, S. G.; Kim, D. M.; Kim, K.; Kim, J.; Kwon, W.-S.; Kim, Y.; Chang, T.; Ree, M. Programmable Digital Memory Characteristics of Nanoscale Thin Films of a Fully π-Conjugated Polymer. *J. Phys. Chem. C* **2009**, *113*, 3855−3861.
(36) Hahm, S. G.; Lee, T. J.; Kim, D. M.; Kwon, W.; Ko, Y.-G.; Michinobu, T.; Ree, M. Electrical Memory Characteristics of Nitrogen-Linked Poly(2,7-carbazole)s. *J. Phys. Chem. C* **2011**, *115*, 21954−21962.
(37) Lee, T. J.; Ko, Y.-G.; Yen, H.-J.; Kim, K.; Kim, D. M.; Kwon, W.; Hahm, S. G.; Liou, G.-S.; Ree, M. Programmable Digital Nonvolatile Memory Behavior of Donor-Acceptor Polyimides Bearing Triphenylamine Derivatives: Effects of Substituents. *Polym. Chem.* **2012**, *3*, 1276−1283.
(38) Song, Y.; Ling, Q. D.; Zhu, C.; Kang, E. T.; Chan, D. S. H.; Wang, Y. H.; Kwong, D.-L. Memory Performance of a Thin-Film Device Based on a Conjugated Copolymer Containing Fluorene and Chelated Europium Complex. *IEEE Electron Device Lett.* **2006**, *27*, 154−156.
(39) Pearson, C.; Ahn, J. H.; Mabrook, M. F.; Zeze, D. A.; Petty, M. C.; Kamtekar, K. T.; Wang, C.; Bryce, M. R.; Dimitrakis, P.; Tsoukalas, D. Electronic Memory Device Based on a Single-Layer Fluorene-Containing Organic Thin Film. *Appl. Phys. Lett.* **2007**, *91*, 123506-1−123506-3.
(40) Ling, Q. D.; Kang, E. T.; Neoh, K. G.; Chen, Y.; Zhuang, X. D.; Zhu, C. X.; Chan, D. S. H. Thermally Stable Polymer Memory Devices Based on a π-Conjugated Triad. *Appl. Phys. Lett.* **2008**, *92*, 143302-1−143302-3.
(41) Ahn, B.; Kim, D. M.; Hsu, J.-C.; Ko, Y.-G.; Shin, T. J.; Kim, J.; Chen, W.-C.; Ree, M. Tunable Film Morphologies of Brush-Linear Diblock Copolymer Bearing Difluorene Moieties Yield a Variety of Digital Memory Properties. *ACS Macro Lett.* **2013**, *2*, 555−560.
(42) Ouisse, T.; Stéfan, O. Electrical Bistability of Polyfluorene Devices. *Org. Electron.* **2004**, *5*, 251−256.
(43) Hahm, S. G.; Ko, Y.-G.; Kwon, W.; Ree, M. Programmable Digital Polymer Memories. *Curr. Opin. Chem. Eng.* **2013**, *2*, 79−87.
(44) Lin, W. P.; Liu, S. J.; Gong, T.; Zhao, Q.; Huang, W. Polymer-Based Resistive Memory Materials and Devices. *Adv. Mater.* **2014**, *26*, 570−606.
(45) Liu, S.-J.; Lin, Z.-H.; Zhao, Q.; Ma, Y.; Shi, H.-F.; Yi, M.-D.; Ling, Q.-D.; Fan, Q.-L.; Zhu, C.-X.; Kang, E.-T. Flash-Memory Effect for Polyfluorenes with On-Chain Iridium(III) Complexes. *Adv. Funct. Mater.* **2011**, *21*, 979−985.
(46) Wang, P.; Liu, S. J.; Lin, Z. H.; Dong, X. C.; Zhao, Q.; Lin, W. P.; Yi, M. D.; Ye, S. H.; Zhu, C. X.; Huang, W. Design and Synthesis of Conjugated Polymers Containing Pt(II) Complexes in the Side-Chain and Their Application in Polymer Memory Devices. *J. Mater. Chem.* **2012**, *22*, 9576−9583.
(47) Terai, M.; Fujita, K.; Tsutsui, T. Electrical Bistability of Organic Thin-Film Device Using Ag Electrode. *Jpn. J. Appl. Phys.* **2006**, *45*, 3754−3757.
(48) Ma, L. P.; Liu, J.; Pyo, S. M.; Yang, Y. Organic Bistable Light-Emitting Devices. *Appl. Phys. Lett.* **2002**, *80*, 362−364.
(49) Ma, L. P.; Liu, J.; Yang, Y. Organic Electrical Bistable Devices and Rewritable Memory Cells. *Appl. Phys. Lett.* **2002**, *80*, 2997-1−2997-3.
(50) Gao, H. J.; Xue, Z. Q.; Wu, Q. D.; Pang, S. J. Structure and Electrical Properties of Ag-Ultrafine-Particle-Polymer Thin Films. *J. Vac. Sci. Technol., B* **1995**, *13*, 1242−1246.
(51) Liu, Z. C.; Xue, F. L.; Su, Y.; Varahramyan, K. Electrically Bistable Memory Device Based on Spin-Coated Molecular Complex Thin Film. *IEEE Electron Device Lett.* **2006**, *27*, 151−153.
(52) Chen, J. S.; Ma, D. G. Performance Improvement by Charge Trapping of Doping Fluorescent Dyes in Organic Memory Devices. *J. Appl. Phys.* **2006**, *100*, 034512-1−034512-4.
(53) Ouyang, M.; Hou, S. M.; Chen, H. F.; Wang, K. Z. A New Organic−-Organic Complex Thin Film with Reproducible Electrical Bistability Properties. *Phys. Lett. A* **1997**, *235*, 413−417.
(54) Michinobu, T. Click-Type Reaction of Aromatic Polyamines for Improvement of Thermal and Optoelectronic Properties. *J. Am. Chem. Soc.* **2008**, *130*, 14074−14075.
(55) Michinobu, T. Click Synthesis of Donor−Acceptor-Type Aromatic Polymers. *Pure Appl. Chem.* **2010**, *82*, 1001−1009.
(56) Michinobu, T.; Seo, C.; Noguchi, K.; Mori, T. Effects of Click Postfunctionalization on Thermal Stability and Field Effect Transistor

Performances of Aromatic Polyamines. *Polym. Chem.* **2012**, *3*, 1427−1435.
(57) Washino, Y.; Murata, K.; Michinobu, T. Postfunctionalization of Aromatic Polyamine by [2 + 2] Cycloaddition of 7,7,8,8-Tetracyanoquinodimethane with Side Chain Alkynes. *Polym. Bull.* **2012**, *69*, 137−147.
(58) Yoon, J.; Kim, K.-W.; Kim, J.; Heo, K.; Jin, K. S.; Jin, S.; Shin, T. J.; Lee, B.; Rho, Y.; Ahn, B.; Ree, M. Small-Angle X-ray Scattering Station 4C2 BL of Pohang Accelerator Laboratory for Advance in Korean Polymer Science. *Macromol. Res.* **2008**, *16*, 575−585.
(59) Lee, B.; Park, Y.-H.; Hwang, Y.; Oh, W.; Yoon, J.; Ree, M. Ultralow-k Nanoporous Organosilicate Dielectric Films Imprinted with Dendritic Spheres. *Nat. Mater.* **2005**, *4*, 147−150.
(60) Lee, B.; Oh, W.; Hwang, Y.; Park, Y.-H.; Yoon, J.; Jin, K. S.; Heo, K.; Kim, J.; Kim, K.-W.; Ree, M. Imprinting Well-Controlled Nanopores in Organosilicate Dielectric Films: Triethoxysilyl-Modified Six-Armed Poly(ε-caprolactone) and Its Chemical Hybridization with Organosilicate Precursor. *Adv. Mater.* **2005**, *17*, 696−701.
(61) Yoon, J.; Jin, K. S.; Kim, H. C.; Kim, G.; Heo, K.; Jin, S.; Kim, J.; Kim, K.-W.; Ree, M. Quantitative Analysis of Lamellar Structures in Brush Polymer Thin Films by Synchrotron Grazing Incidence X-ray Scattering. *J. Appl. Crystallogr.* **2007**, *40*, 476−488.
(62) Yoon, J.; Lee, S. W.; Choi, S.; Heo, K.; Jin, K. S.; Jin, S.; Kim, G.; Kim, J.; Kim, K.-W.; Kim, H.; Ree, M. Two-Dimensionally Well-Ordered Multilayer Structures in Thin Films of a Brush Polypeptide. *J. Phys. Chem. B* **2008**, *112*, 5338−5349.
(63) Kim, G.; Park, S.; Jung, J.; Heo, K.; Yoon, J.; Kim, H.; Kim, I. J.; Kim, J. R.; Lee, J. I.; Ree, M. Novel Brush Polymers with Phosphorylcholine Bristle Ends: Synthesis, Structure, Properties, and Biocompatibility. *Adv. Funct. Mater.* **2009**, *19*, 1631−1644.
(64) Park, B.-J.; Rah, S.-Y.; Park, Y.-J.; Lee, K.-B. PLS Bending Magnet X-Ray Beamline 3C2. *Rev. Sci. Instrum.* **1995**, *66*, 1722−1724.
(65) Bolze, J.; Kim, J.; Huang, J.-Y.; Rah, S.; Youn, H. S.; Lee, B.; Shin, T. J.; Ree, M. Current Status of the Synchrotron Small-Angle X-Ray Scattering Station BL4C1 at the Pohang Light Source. *Macromol. Res.* **2002**, *10*, 2−12.
(66) Oh, W.; Hwang, Y.; Shin, T. J.; Lee, B.; Kim, J.-S.; Yoon, J.; Brennan, S.; Mehta, A.; Ree, M. Synchrotron X-ray Reflectivity Studies of Nanoporous Oganosilicate Thin Films with Low Dielectric Constants. *J. Appl. Crystallogr.* **2007**, *40*, s626−s630.
(67) Parratt, L. G. Surface Studies of Solids by Total Reflection of X-rays. *Phys. Rev.* **1954**, *95*, 359−369.
(68) Bolze, J.; Ree, M.; Youn, H. S.; Chu, S.-H.; Char, K. Synchrotron X-ray Reflectivity Study on the Structure of Templated Polyorganosilicate Thin Films and Their Derived Nanoporous Analogs. *Langmuir* **2001**, *17*, 6683−6691.
(69) Hwang, Y.; Heo, K.; Chang, C. H.; Joo, M. K.; Ree, M. Synchrotron X-ray Reflectivity Study of High Dielectric Constant Alumina Thin Films Prepared by Atomic Layer Deposition. *Thin Solid Films* **2006**, *510*, 159−163.
(70) Campbell, A. J.; Bradley, D. D. C.; Lidzey, D. G. Space-Charge Limited Conduction with Traps in Poly(phenylene vinylene) Light Emitting Diodes. *J. Appl. Phys.* **1997**, *82*, 6326−6342.
(71) Jensen, K. L. Electron Emission Theory and Its Application: Fowler−Nordheim Equation and beyond. *J. Vac. Sci. Technol., B* **2003**, *21*, 1528−1544.
(72) Mark, P.; Helfrich, W. Space-Charge-Limited Currents in Organic Crystals. *J. Appl. Phys.* **1962**, *33*, 205−215.
(73) Laurent, C.; Kay, E.; Souag, N. Dielectric Breakdown of Polymer Films Containing Metal Clusters. *J. Appl. Phys.* **1998**, *64*, 336−343.